

Impact of Nuclear Effects in the Measurement of Neutrino Oscillation Parameters

Davide Meloni

Dipartimento di Fisica "E. Amaldi", Universitá degli Studi Roma Tre, Via della Vasca Navale 84, 00146 Roma

E-mail: meloni@fis.uniroma3.it

Abstract. In recent years the experimental study of neutrino oscillations has much contributed to our knowledge of particle physics by establishing non vanishing neutrino masses and by measuring or constraining the corresponding mixing angles. Within the domain of neutrino oscillations, the main goal of the next generation of facilities is the measurement of the mixing angle θ_{13} and the observation of leptonic CP violation, for which we have no hints at the moment. We discuss more in detail how various models of neutrino-nucleus cross section affect the forecasted precision measurement of θ_{13} and the CP violating phase δ [1].

Contribution to NUFAC 11, XIIIfth International Workshop on Neutrino Factories, Super beams and Beta beams, 1-6 August 2011, CERN and University of Geneva (Submitted to IOP conference series)

1. Summary of the charged current neutrino-nucleus cross sections

In the quasi-elastic regime (QE), the doubly-differential cross section, in which a neutrino carrying initial four-momentum $k = (E_\nu, \mathbf{k})$ scatters off a nuclear target to a state of four-momentum $k' = (E_\ell, \mathbf{k}')$ can be written in Born approximation as follows:

$$\frac{d^2\sigma}{d\Omega dE_\ell} = \frac{G_F^2 V_{ud}^2}{16 \pi^2} \frac{|\mathbf{k}'|}{|\mathbf{k}|} L_{\mu\nu} W_A^{\mu\nu}, \quad (1)$$

where G_F is the Fermi constant and V_{ud} is the CKM matrix element coupling u and d quarks. The leptonic tensor is completely determined by lepton kinematics, whereas the nuclear tensor $W_A^{\mu\nu}$, containing all the information on strong interactions dynamics, describes the response of the target nucleus, $W_A^{\mu\nu} = \sum_X \langle 0 | J_A^{\mu\dagger} | X \rangle \langle X | J_A^\nu | 0 \rangle \delta^{(4)}(p_0 + q - p_X)$, where $|0\rangle$ and $|X\rangle$ are the initial and final hadronic states carrying four momenta p_0 and p_X and J_A^μ is the nuclear electroweak current operator; the sum includes all hadronic final states. In the impulse approximation (IA) scheme, the nuclear current can be written as a sum of one-body currents, i.e. $J_A^\mu \rightarrow \sum_i J_i^\mu$, while the final state reduces to the direct product of the hadronic state produced at the weak vertex (with momentum \mathbf{p}') and that describing the $(A - 1)$ -nucleon residual system, with momentum \mathbf{p}_R : $|X\rangle \rightarrow |i, \mathbf{p}'\rangle \otimes |\mathcal{R}, \mathbf{p}_R\rangle$.

1.1. The Spectral Function approach

Following Ref. [2], the final expression of the hadronic tensor can be cast in the following form:

$$W_A^{\mu\nu} = \frac{1}{2} \int d^3 p dE P(\mathbf{p}, E) \frac{1}{4E_{|\mathbf{p}|} E_{|\mathbf{p}+\mathbf{q}|}} W^{\mu\nu}(\tilde{p}, \tilde{q}) , \quad (2)$$

where $E_{\mathbf{p}} = \sqrt{|\mathbf{p}|^2 + m_N^2}$ and the function $P(\mathbf{p}, E)$ is the target *Spectral Function*, i.e. the probability distribution of finding a nucleon with momentum \mathbf{p} and removal energy E in the target nucleus. The quantity $W^{\mu\nu}$ is the tensor describing the weak interactions of the i -th nucleon in free space; the effect of nuclear binding of the struck nucleon is accounted for by the replacement $q = (\nu, \mathbf{q}) \rightarrow \tilde{q} = (\tilde{\nu}, \mathbf{q})$ with $\tilde{\nu} = E_{|\mathbf{p}+\mathbf{q}|} - E_{|\mathbf{p}|}$. The second argument in the hadronic tensor is $\tilde{p} = (E_{|\mathbf{p}|}, \mathbf{p})$.

1.2. The Relativistic Fermi Gas

The RFG [3] model, widely used in MonteCarlo simulations, provides the simplest form of the Spectral Function, $P_{RFGM}(\mathbf{p}, E) = \left(\frac{6\pi^2 A}{p_F^3} \right) \theta(p_F - |\mathbf{p}|) \delta(E_{\mathbf{p}} - E_B + E)$, where p_F is the Fermi momentum and E_B is the average binding energy, introduced to account for nuclear binding. Thus, in this model p_F and E_B are two parameters that are *adjusted* to reproduce the experimental data. For oxygen, the analysis of electron scattering data yields $p_F = 225$ MeV and $E_B = 25$ MeV.

1.3. The Relativistic Mean Field approach

Within the Relativistic Mean Field approximation we refer to the model described in [4], where, like in the previous cases, the nuclear current is written as a sum of single-nucleon currents. The wave functions for the target and the residual nuclei are described in terms of an independent-particle model. Then, the transition matrix elements can be cast in the following form:

$$J_N^\mu(\omega, \vec{q}) = \int d\vec{p} \bar{\psi}_F(\vec{p} + \vec{q}) \hat{J}_N^\mu(\omega, \vec{q}) \psi_B(\vec{p}) , \quad (3)$$

where ψ_B and ψ_F are the wave functions for initial bound and final outgoing nucleons, respectively, and \hat{J}_N^μ is the relativistic current operator. In particular, the relativistic bound-state wave functions (for both initial and outgoing nucleons) are obtained as a solution of the Dirac equation, in the presence of the same relativistic nuclear mean field potential, derived from a Lagrangian containing σ , ω and ρ mesons.

1.4. The Random Phase Approximation

The last model we want to take into account has been introduced in [5], where the hadronic tensor is expressed in terms of the nuclear response functions treated in the Random Phase Approximation (RPA). The response functions are related to the imaginary part of the corresponding full polarization propagators and the introduction of the RPA approximation means that the polarization propagators are the solutions of integral equations involving the bare propagators and the effective interaction between particle-hole excitations. Within this formalism, the authors of [5] were able to show that multinucleon terms sizably increase the genuine charged current QE cross section in such a way to reproduce the MiniBooNE results [6]. The mechanism responsible for the enhancement that brings the theoretical cross section into agreement with the data is multi nucleon knock out, leading to two particle-two hole (2p2h) nuclear final states. In the following, we will refer to this “generalized” QE cross section as RPA-2p2h whereas we adopt the short RPA for the genuine QE cross section.

1.5. Comparison of the cross sections

To summarize this section, we present in Fig.1 a comparison of the five total QE cross sections for the $\nu_\mu^{16}O \rightarrow \mu^- X$ process (left panel) and $\bar{\nu}_\mu^{16}O \rightarrow \mu^+ X$ (right panel), in the energy range $E_\nu \sim [0, 0.75]$ GeV. The curves have been computed using the dipole structure of the form factors and, in particular, a value of the axial mass close to $m_A \sim 1$ GeV. As it can be easily

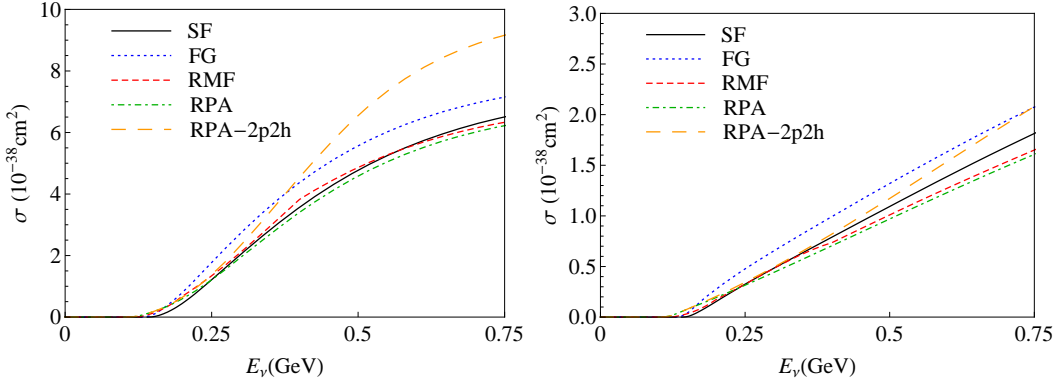


Figure 1. Total charged current QE cross sections for the $\nu_\mu^{16}O \rightarrow \mu^- X$ (left panel) and $\bar{\nu}_\mu^{16}O \rightarrow \mu^+ X$ (right panel) processes in the energy range $E_\nu \sim [0, 0.75]$ GeV.

seen in the left panel, the RFG prediction sizably overestimates the SF, RMF and RPA results by roughly 15%, a fact that is well known to happen also for many other models with a more accurate description of the nuclear dynamics than the RFG approach. On the other hand, the inclusion of 2p2h contributions largely enhances the QE cross section in the RPA approximation for energies above ~ 0.5 GeV, although it is smaller than the RFG at smaller energies. For antineutrinos (right panel) the observed pattern is almost the same.

2. The impact on the $(\theta_{13}-\delta)$ measurement

To estimate the impact of different models of the cross section on the measurement of θ_{13} and leptonic CP violation we choose a $\gamma = 100$ β -Beam facility as a representative example because the neutrino flux from such a facility spans up to ~ 0.7 GeV with the peak around 0.3 GeV and is thus mostly sensitive to the quasielastic region explored here. Details of the detector response can be found in Ref. [7]. It is important to notice that we are only using the quasielastic contribution to the neutrino cross section depicted in Fig.1. As an illustration we have focused on the dependence on the nuclear model adopted of two different observables, namely the *CP* and θ_{13} *discovery potentials*, defined as the values of the CP-violating phase δ_{CP} and θ_{13} for which respectively the hypothesis of CP conservation $\delta_{CP} = 0, \pm\pi$ or $\theta_{13} = 0$ can be excluded at 3σ after marginalizing over all other parameters. The CP discovery potential is shown in the left panel of Fig.2, where we superimposed the results obtained using the RFG cross section and the SF, RMF and RPA calculations. We clearly see that, for $\delta_{CP} \sim \pm 90^\circ$ (where the sensitivity is maximal) the RFG model gives a prediction which is around a factor 2 better than the SF, RMF and RPA models (which, as expected, behave almost in the same way) in $\sin^2 2\theta_{13}$ and around a 40% better than the RPA-2p2h. This is not surprising because the β -Beam facility used in our simulations mainly probes energies smaller than 0.5 GeV, where the RFG is still larger than any other model (see Fig.1). For the other points in the parameter space, the difference is less evident but still significant. The difference in the sensitivity to θ_{13} can be seen in the right panel of Fig. 2 where we show the results in the $(\sin^2 2\theta_{13}, \delta_{CP})$ -plane. In this case the predictions of the SF, RMF and RPA models differ by up to a factor of $\sim 60\%$ compared to the RFG model for $\delta_{CP} \sim \pm 90^\circ$ while the difference is less pronounced for $\delta_{CP} \sim 0^\circ$. The RPA-2p2h results are

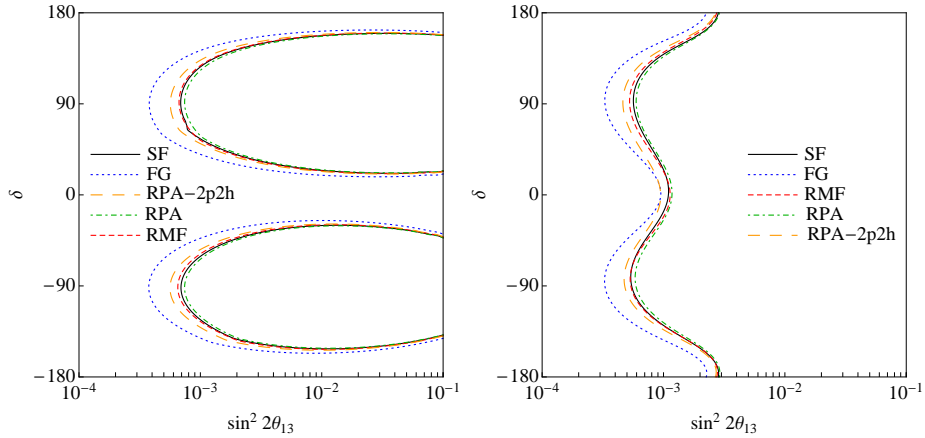


Figure 2. Left panel: CP discovery potential in the $(\theta_{13}, \delta_{CP})$ plane. Solid lines refer to the SF model, dotted lines to the RFG, short-dashed lines to the RMF, dot-dashed to RPA and long-dashed to RPA-2p2h. Right panel: θ_{13} discovery potential.

more similar to the RFG for $\delta_{CP} \sim 0^\circ$ and to the other models for $\delta_{CP} \sim 180^\circ$. This is also evident in the right panel where we show the CP fraction.

Finally, it is interesting to comment on the effect of using different nuclear models also in the simultaneous determination of θ_{13} and δ_{CP} . We have performed such an analysis for the input value $(\theta_{13}, \delta_{CP}) = (0.9^\circ, 30^\circ)$ (not including degenerate solutions coming from our ignorance of the octant of θ_{23} [8] and in the neutrino mass ordering) finding that, using the RFG and RPA-2p2h models, we are able to reconstruct the true values of θ_{13} and δ_{CP} within reasonable uncertainties, whereas with the other models we can only measure two distinct disconnected regions (the fake one around the value of θ_{13} and $\delta_{CP} \sim 180^\circ$), which worsen the global sensitivity on those parameters. In conclusion, we have analyzed the impact of five different theoretical models for the neutrino-nucleus charged current QE cross sections on the forecasted sensitivity of the future neutrino facilities to the parameters θ_{13} and δ_{CP} . We have found that the sensitivities computed with the FG are better, by up to a factor of 2, with respect to the other models.

Acknowledgments

We acknowledge MIUR (Italy), for financial support under the contract PRIN08.

References

- [1] E. Fernandez-Martinez, D. Meloni, Phys. Lett. **B697**, 477-481 (2011). [arXiv:1010.2329 [hep-ph]].
- [2] O. Benhar, N. Farina, H. Nakamura, M. Sakuda and R. Seki, Phys. Rev. D **72**, 053005 (2005) [arXiv:hep-ph/0506116]; O. Benhar and D. Meloni, Nucl. Phys. A **789**, 379 (2007) [arXiv:hep-ph/0610403]; O. Benhar and D. Meloni, Phys. Rev. D **80**, 073003 (2009) [arXiv:0903.2329 [hep-ph]].
- [3] R. A. Smith and E. J. Moniz, Nucl. Phys. B **43** (1972) 605 [Erratum-ibid. B **101** (1975) 547].
- [4] C. Maieron, M. C. Martinez, J. A. Caballero and J. M. Udias, Phys. Rev. C **68**, 048501 (2003) [arXiv:nucl-th/0303075]; M. C. Martinez, P. Lava, N. Jachowicz, J. Ryckebusch, K. Vantournhout and J. M. Udias, Phys. Rev. C **73**, 024607 (2006) [arXiv:nucl-th/0505008].
- [5] M. Martini, M. Ericson, G. Chanfray and J. Marteau, Phys. Rev. C **80**, 065501 (2009) [arXiv:0910.2622 [nucl-th]]; M. Martini, M. Ericson, G. Chanfray and J. Marteau, Phys. Rev. C **81** (2010) 045502 [arXiv:1002.4538 [hep-ph]].
- [6] A. A. Aguilar-Arevalo *et al.* [MiniBooNE Collaboration], Phys. Rev. D **81** (2010) 092005 [arXiv:1002.2680 [hep-ex]].
- [7] J. Burguet-Castell, D. Casper, E. Couce, J. J. Gomez-Cadenas and P. Hernandez, Nucl. Phys. B **725**, 306 (2005) [arXiv:hep-ph/0503021].
- [8] D. Meloni, Phys. Lett. **B664**, 279-284 (2008). [arXiv:0802.0086 [hep-ph]].